

## **Carbon Monoxide Adsorption at Polycrystalline Copper in Aqueous Phosphate Buffered Solution: Linearly-Adsorbed CO**

**Jumat Salimon and Maher Kalaji\***

School of Chemical Sciences and Food Technology, Universiti Kebangsaan Malaysia, 43600 Bangi, Selangor DE, Malaysia

\* Department of Chemistry, University of Wales, Bangor, UK LL57 2UW

**Abstract** : The electrochemical adsorption of carbon monoxide at polycrystalline copper was carried out in aqueous phosphate buffered solutions. The results showed that the type of CO adsorption process depended on the state of the copper surface, either with or without potential polarization process. Adsorbed CO was not observed when no cathodic potential was applied to the electrode surface. Linearly adsorbed carbon monoxide, Cu-CO<sub>L</sub> appeared immediately after the surface was polarized at the starting applied potential, E<sub>ASP</sub> of high cathodic potential. It appeared in a narrow potential range from -1.5 to -1.0 V. The IR band of Cu-CO<sub>L</sub> at 2078 cm<sup>-1</sup> showed potential-dependent frequency shift around 15 cm<sup>-1</sup>/V. No Cu-CO<sub>L</sub> was observed at potential below -1.0 V. The interaction of CO on copper surface results from the adsorption of CO in molecular form and occurs at more than one binding sites.

**Abstrak** : Penjerapan karbon monoksida secara elektrokimia di atas kuprum polikristal telah dikaji dalam larutan tampan fosfat berakuas. Hasil kajian menunjukkan bahawa bentuk penjerapan CO bergantung kepada keadaan permukaan kuprum, samada mengalami atau tidak, proses polarisasi keupayaan. CO terjerap tidak wujud apabila permukaan kuprum tidak dikenakan proses polarisasi keupayaan katodik. Karbon monoksida terjerap secara lurus, Cu-CO<sub>L</sub> wujud serta merta apabila permukaan elektrod mengalami polarisasi keupayaan permulaan awal, E<sub>ASP</sub> pada keupayaan katodik yang tinggi. Ia wujud dalam julat keupayaan yang kecil dari -1.5 hingga -1.0 V. Nombor gelombang puncak inframerah Cu-CO<sub>L</sub> pada 2078 cm<sup>-1</sup> menunjukkan anjakan frekuensi kebergantungan-keupayaan sebanyak 15 cm<sup>-1</sup>/V. Tiada Cu-CO<sub>L</sub> diperhatikan pada keupayaan yang lebih rendah dari -1.0 V. Interaksi CO di atas permukaan kuprum adalah hasil dari penjerapan CO dalam bentuk molekul dan terjadi dalam lebih dari satu bentuk pengikatan.

Received : 30.04.02; accepted : 7.01.03

### **Introduction**

In aqueous solution particularly, carbon monoxide reacts as a soluble compound. In the presence of an electrode potential, carbon monoxide reacts and adsorbs on the surface. Carbon monoxide may adsorb either in a molecular form or in a dissociative fashion where in some cases both states coexist on particular surface planes and over specific ranges of temperature, depending on the metal surface. For the majority of the transition metals, the nature of the adsorption (molecular or dissociative) is very sensitive to the surface temperature and surface structure; for example the presence of any lower coordination sites such as step and defects sites, and a mixture of a variety of surface structure as in polycrystalline surfaces [1]. Molecularly chemisorbed CO has been found to bind in various ways to single crystal metal surfaces, analogous to its behaviour in isolated metal carbonyl complexes [2]. Linear or terminal binding sites of low coordination involve chemisorption of a single CO molecule onto one metal substrate atom, M-CO, which has the highest energy and heat of adsorption. Bonding in high coordination binding sites on the other hand, such as to 2-fold bridge and 3-fold hollow sites shows

high stability. Consequently, as the number of metal atoms to which the carbon is coordinated increases, there is a corresponding increase in the M-CO bond order and a reduction in the C-O bond order [1].

However, CO does not necessarily prefer to bind to the highest available coordination site. The fact that there are 3-fold hollow sites on many surfaces of face centered cubic materials does not mean that CO will necessarily adsorb to these sites. Moreover, the preferred site may still be a terminal or a 2-fold bridging site, and the site which is occupied, may change with surface coverage, temperature or applied potential. The energy difference between the various adsorption sites available for molecular CO chemisorptions appears therefore to be very small [3]. Adsorbed carbon monoxide usually gives rise to strong absorption bands in both the infrared (IR) and electron energy loss spectroscopy (EELS) spectra in the νC≡O stretching frequency region (2200 -1800 cm<sup>-1</sup>) [4]. The metal-carbon stretching mode (400 -100 cm<sup>-1</sup>) is also accessible to EELS. The interpretation of spectra of CO as an adsorbed surface species draws heavily upon IR spectra from related inorganic cluster and coordination complexes with the structure of such complexes usually being available from x-ray single crystal diffraction measurements. Nevertheless the IR

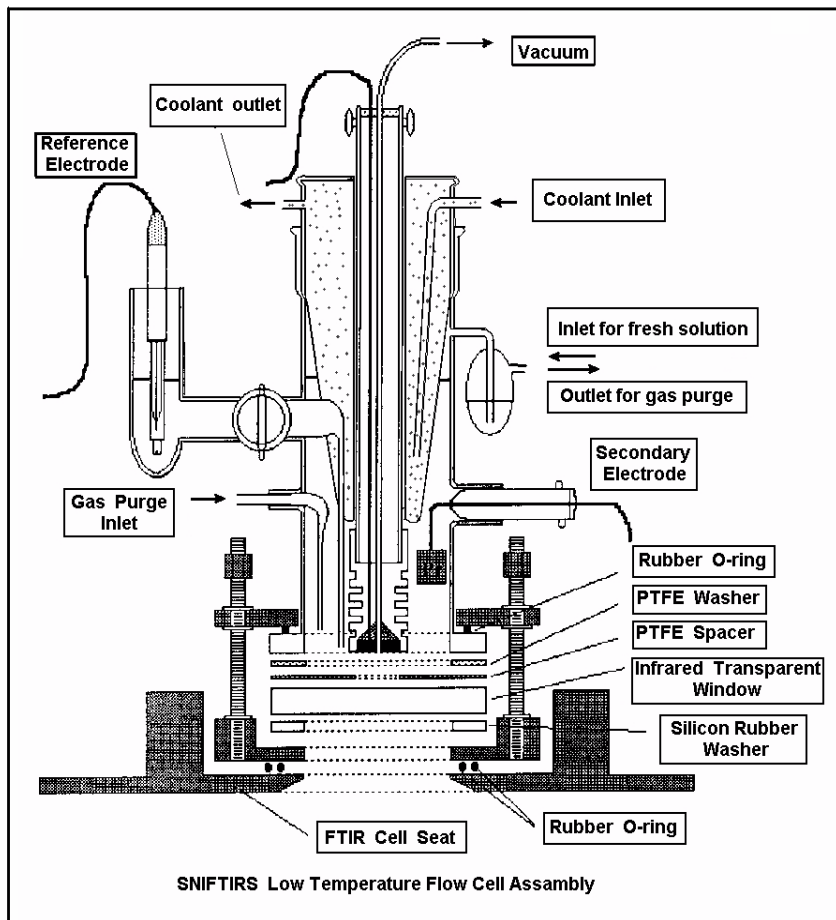


Figure 1: Schematic diagram of FTIR *in situ* measurement cell set up.

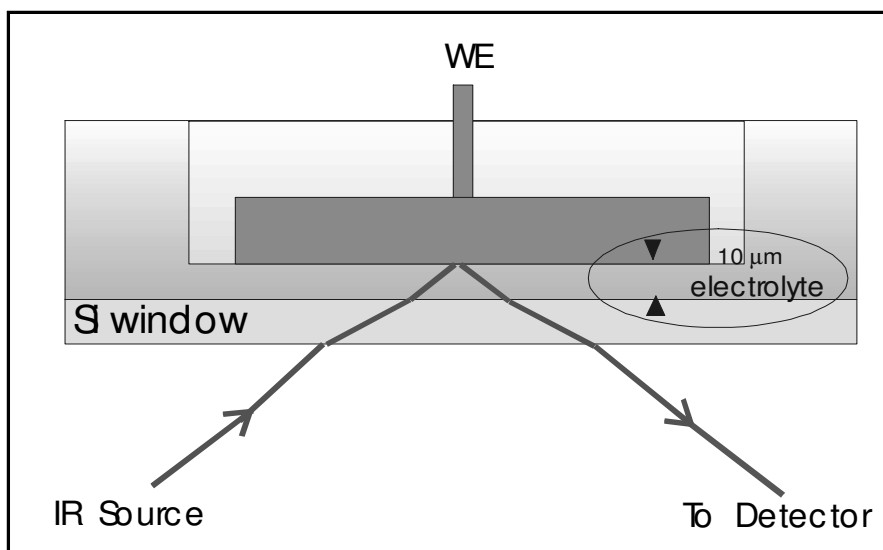


Figure 2: An electrolyte thin layer for the *in situ* measurement.

spectra of  $\nu\text{C}\equiv\text{O}$  stretching frequency can provide a good indication of the surface coordination of the molecule as a rough guideline.

In this work, the adsorption of CO on polycrystalline copper electrode was investigated in phosphate buffered solution. The spectroscopic properties of the adsorbed CO on Cu were investigated as a function of applied starting potential ( $E_{\text{ASP}}$ ) and CO surface coverage. Using *in situ* IR measurements, we report the existence of the adsorbed carbon monoxide on the polycrystalline copper electrode surface, as the applied potentials were varied. The behavior of the bands demonstrates a change in CO binding state and surface coverage as the  $E_{\text{ASP}}$  was changed.

### Experimental

Phosphate buffer solution was used as supporting electrolyte. A mixture of reagent grade chemicals of 0.1M potassium dihydrogen phosphates,  $\text{KH}_2\text{PO}_4$  (>99.5%) and 0.1M dipotassium hydrogen phosphates,  $\text{K}_2\text{HPO}_4$  (>99%) in 2:1 volume ratio has been used to prepare a 6.8 pH buffer solution. Solutions were prepared from ultra-pure water (18 M $\Omega$ ) obtained using an Elgastat UHQII MKII purification system. The copper electrode used was electrochemically polished. First, the electrode was polished with successively down graded sizes up to 0.05  $\mu\text{m}$  alumina powder, rinsed with distilled water and cleaned in ultrasonic bath for 5 min. The electrode was then immersed in freshly concentrated  $\text{H}_3\text{PO}_4$  (85%). A constant current of 0.02 mA was applied for 8 min with Pt as a counter electrode to perform electropolishing. The electrode was then rinsed with double distilled water and cleaned in an ultrasonic bath for 5 min.

The spectroscopic experiments were carried out in an *in situ* three electrode cell with a Pt ring and a saturated calomel electrode as counter and reference electrode, respectively as shown in Figure 1. The IR spectra were recorded in a staircase mode using a fully evacuated FTIR spectrometer (Bruker IFS-113V) fitted with a mercury-cadmium-telluride (MCT) photoconductive detector cooled at 77 °K (using liquid nitrogen), *p*-polarizer and Ge/KBr beam splitter. The optics bench was fully evacuated. Medium resolution of 4  $\text{cm}^{-1}$  was sufficient for the Subtractively Normalized Interfacial Fourier Transform Infrared Spectroscopy, SNIFTIRS experiments and this was attainable throughout the mid-IR region, with a maximum aperture of 10 mm diameter and medium scanner speed of 6 kHz/sec. A thin layer of supporting electrolyte is required to perform the *in situ* IR measurement. A typical thin layer of CO saturated electrolyte was formed by pushing a flat working electrode against the IR window as shown in Figure 2. SNIFTIR spectra collection was performed at 200 interferograms in a staircase mode. The potential generated by Hi-Tek

DT-2101 potentiostat and PP-R1 waveform generator, was changed by 100 mV during each step which was run under OPUS 3.0, which enables voltage 'steps' to be programmed. A time delay was introduced after any change in voltage and before the collection of spectra was started, in order to allow the electrochemical system to reach a stable semi-steady state.

In SNIFTIRS, a sophisticated FTIR spectrometer is normally required for work at the electrode/electrolyte solution interface. The instrument should be able to allow alternating access to several memories for adding the interferograms at several different potential limits. The potential of the working electrode is applied in "staircase mode" which consists of successive potential steps. The spectra obtain from this technique can be represented as normalized difference spectra ( $\Delta R/R$ ) in two ways. The first method is as the dynamic reference normalization (DRN) method where it compares the spectra taken at various potentials at the previous potentials. This operation helps to distinguish between the electrochemical processes occurring after a particular potential step [5]. It also provides an "instantaneous picture" of the system after each potential step. The second method consists of correlating successive spectra ( $R_n$ ) with a single reference spectrum, usually the spectrum taken at the initial potential ( $R_1$ ), which is giving the normal background without any perturbation effect [6]. This particular normalization is shown by the following equation:

$$\Delta R/R = [R_n - R_1] / R_1 = [R_n / R_1] - 1$$

This processing method of the raw spectra resulting spectra contain the accumulation of the vibrational changes occurred since the application of the first potential spectrum; thus provides an accumulative spectrum. This would be equivalent to a successive addition of all DRN spectra up to the DRN spectra obtained at a specific potential. This normalization is known as the static reference normalization (SRN).

### Results and discussion

#### *In situ* FTIR – linearly adsorbed CO

All spectra presented here are normalized using SRN method. The band showing downward is representing an increment in spectrum intensity and the band pointing upward is representing decreasing in band intensity. The electrochemical behavior of copper electrode in CO saturated phosphate buffered solution before the IR measurement has been discussed in detail [7]. For the *in situ* measurements, the removal of water vapor and  $\text{CO}_2$  in the optics bench of the FTIR is crucial since this exhibit strong IR absorbance. Evacuation of the spectrometer bench for two hours produced a significant improvement in the interferometer stability and the IR spectrum produced. This was due to the IR cell

was firmly hold as well as removing atmospheric component absorption from the spectra.

The phosphate buffered solution was first degassed with purified  $N_2$  for 30 minutes in order to remove oxygen and  $CO_2$ . After that, the solution was saturated with purified CO (15 min bubbling time), the electrode was then introduced into the solution and a potential, applied starting potential,  $E_{ASP}$ , was applied. Spectral collection was performed after the observed current had stabilized which normally took 30 s. The potential was then stepped in 0.1 V increments to  $-0.7$  V.  $E_{ASP}$  values were ranged from  $-1.5$  V to  $-0.8$  V.

Figure 3 shows the results obtained from 14 sets of experiments. The first set, Figure 3 ( $a_1$ - $a_7$ ) show the spectra obtained from  $^{12}CO$ -saturated solutions. Each spectrum was calculated by subtracting the spectrum obtained at  $-0.8$  V (reference spectrum at reference potential,  $E_{ref} = -0.8$  V) in each set, from the spectrum collected at  $E_{ASP}$ . The upward or positive bands correspond to increased absorbance at reference potential or decrease absorbance at  $E_{ASP}$ , whereas bands pointing downward or negative bands indicate increased absorbance at  $E_{ASP}$ . A monopolar band is observed at  $2085\text{ cm}^{-1}$  (at  $-1.2$  V) that shifts

with potential to  $2078\text{ cm}^{-1}$  at  $-1.5$  V. This band is neither observed in  $N_2$ -saturated solution under the same conditions nor in  $^{12}CO$ -saturated solution when  $s$ -polarized light was used. From the surface selection rules, it is clear that the species responsible for this absorption is an adsorbed species and as expected it is assigned to linear bonded CO on copper surface,  $Cu-^{12}CO_L$ . The band position is in agreement with  $\nu C\equiv O$  stretching frequency of adsorbed CO on Cu, which lies in the frequency range of  $1990$  to  $2100\text{ cm}^{-1}$  for linearly adsorbed CO on thin Cu films [8-10] and on Cu(100) at  $2070$  to  $2090\text{ cm}^{-1}$  [11,12]. The adsorption of CO must be responsible for the observed negative shifts in the onset of hydrogen evolution reaction, HER as indicated by voltammogram as previously reported [7]. It is worth to note that when mechanically polished electrode was used, no adsorbed CO was observed under the same experimental conditions (spectra not shown). The results show that the electrode surface condition plays an important role for the adsorption of CO at copper. It may relate to the existence of competing pre-adsorbed anions species on the electrode surface

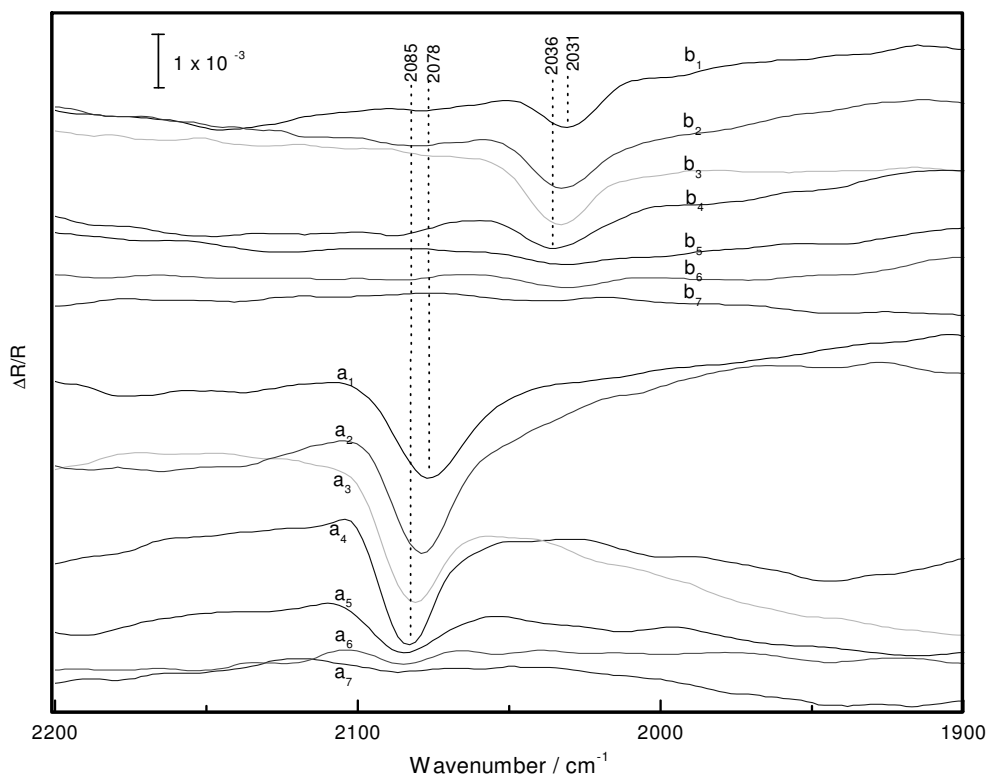


**Figure 3:** SNIFTIR spectra obtained from a  $^{12}CO$  ( $a_1$ - $a_7$ ) and  $^{13}CO$ -saturated ( $b_1$ - $b_7$ ) buffered phosphate solution at each  $E_{ASP}$  at  $0^\circ C$ . Spectra shown are at (1)  $E_{ASP} = -1.5$  V to (7)  $E_{ASP} = -0.9$  V. The spectra are normalized relative to  $E_{ref} = -0.8$  V of each set.

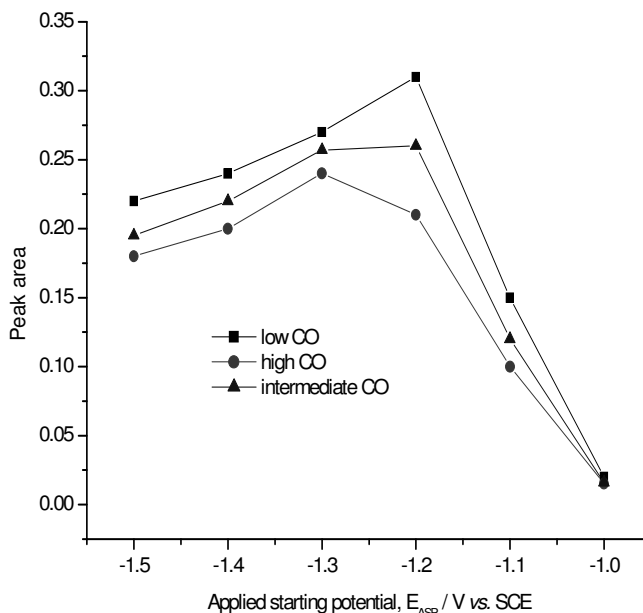
that block the CO adsorption process. This is in agreement with the observation of the pre-adsorbed hydroxyl ions at non-polarized electrode surface as has been reported previously [13].

The other spectra shown in Figure 3 (b<sub>1</sub>-b<sub>7</sub>) were obtained when <sup>13</sup>CO was used. The other experimental conditions were the same as those used with <sup>12</sup>CO. Linear bonded <sup>13</sup>CO, Cu-<sup>13</sup>CO<sub>L</sub> is observed at 2036 cm<sup>-1</sup> (at -1.2 V) and shifted to 2031 cm<sup>-1</sup> (at -1.5 V Figure 3 b<sub>1</sub>). The frequency shift with potential is clearly due to the same phenomenon as with <sup>12</sup>CO. The isotopic frequency shift (49 cm<sup>-1</sup>) is due to the differences in the reduced mass of the molecule [14, 15]. Again this is well in agreement with other reports on <sup>13</sup>CO isotopic labeling effect for adsorbed <sup>13</sup>CO on Cu(111) and Cu(110) where the band appears at 2030 cm<sup>-1</sup> [16, 17] and on other metal such as Pt(111) at 2035 cm<sup>-1</sup> [18, 19]. In the present work, the potential-dependent frequency shift was observed around 15 cm<sup>-1</sup>/V. However, Pritchard and Sims [10] reported that the stretching frequency of adsorbed CO on Cu did not exhibit a large shift with CO surface coverage, and also with electrode potential as reported by Hayden *et al.* [20]. This is due to the chemical and dipole-coupling shifts, which have the opposite effect on the CO frequency, are nearly the same. Nevertheless, the results obtained here show a red shift with increasing negative potential. This can be explained in terms of the partial cancellation of the blue coupling shift and the red chemical shift, as suggested by Hayden *et al.* [20] and by Woodruff *et al.* [21].

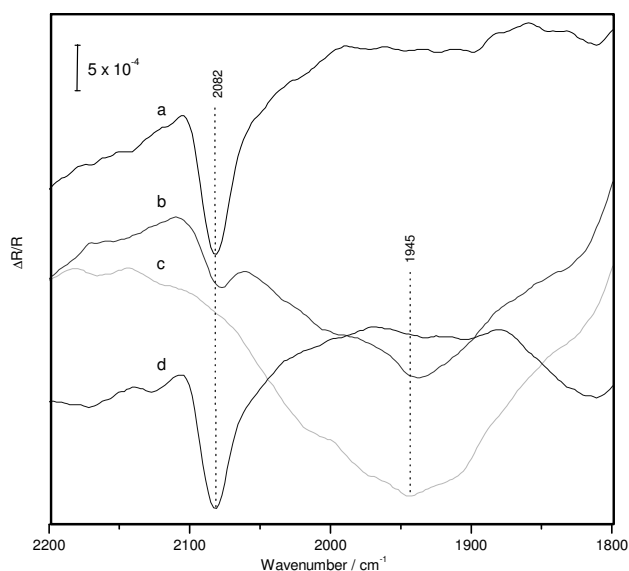
#### The amount of Cu-CO<sub>L</sub> as a function of potential and concentration

Figure 4 shows the integrated peak area for the bands observed from experiments carried out under the same condition as those used to produce the spectra in Figure 3a, except that the CO bubbling time was varied. One set of data was obtained for short bubbling time (3 min, square curve) and the other set was obtained at long bubbling time (30 min, round curve). It is clear from the round curve that for CO saturated solutions, the amount of CO adsorbed linearly at the surface, increases as the initial applied potential, E<sub>ASP</sub>, is changed from -1.5 V to -1.3 V, after which it decreases rapidly. It is important to point out at this stage that the analysis has been done when E<sub>ASP</sub> was varied and not when the initial E<sub>ASP</sub> potential was stepped to different values. The later situation is the same as shown in Fig. 3. Unexpectedly, when the concentration of CO was decreased (3 min bubbling time), the amount of linear bonded CO increased compared to the saturated solution. This indicates that for linearly bonded CO is inversely proportional to the concentration of CO in solution. Figure 5 shows a comparison between the spectrum obtained at E<sub>ASP</sub> = -1.3 V (Fig 5a) and

the spectra obtained at -1.3 V after E<sub>ASP</sub> was set at -1.4 V (Fig. 5b) and -1.5 V (Fig. 5c). The spectra

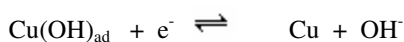


**Figure 4 :** Integrated peak area of Cu-CO<sub>L</sub> at E<sub>ASP</sub> as the SNIFTIR spectra are normalized relative to E<sub>ref</sub> = -0.8 V at each set.



**Figure 5:** Comparison of the Cu-CO<sub>L</sub> at -1.3 V obtained from different E<sub>ASP</sub> values, (a) E<sub>ASP</sub> = -1.3 V, (b) E<sub>ASP</sub> = -1.4 V, (c) E<sub>ASP</sub> = -1.5 V and (d) another E<sub>ASP</sub> = -1.3 V, as the spectra are normalized relative to E<sub>ref</sub> = -0.8 V of each sets.

clearly show that the amount of linearly bonded CO at  $-1.3$  V decreases if  $E_{ASP}$  was more negative than  $-1.3$  V. A new absorbance is observed, when the data is treated in this way, at around  $1945\text{ cm}^{-1}$ . Its intensity is at its highest when  $E_{ASP} = -1.5$  V and completely disappears at  $E_{ASP} = -1.3$  V. It is very tempting to assign this absorbance to Cu-H, which is reported to be at  $1940\text{ cm}^{-1}$  [22]. It has been postulated that at negative potentials, metallic copper is formed according to the following equation [23-26];



Others suggested [27] the formation of a hydrogen adsorbate;



Therefore in the work reported here, it may be concluded that after the reduction of the surface hydroxide layer, Cu-H can be produced in competition with CO adsorption. At potentials more negative than  $-1.3$  V, Cu-H can be produced and compete with the adsorption of CO on the clean surface. However, this conclusion does not fully explain the following observation. As the potential was stepped from  $E_{ASP} = -1.5$  V to  $-1.3$  V no Cu-CO<sub>L</sub> was observed at  $-1.3$  V. However if the potential was stepped from  $E_{ASP} = -1.4$  V to  $-1.3$  V, a small Cu-CO<sub>L</sub> band was observed. The main difference in the experiment is the time taken to reach  $-1.3$  V. Evidence will be provided in the future discussion dealing with bridge bonded CO to show that the effect of polarization time and the concentration of dissolved CO are to increase CO surface coverage,  $\theta_{\text{CO}}$  and hence lead to the transformation to bridge bonded CO.

Figure 6 shows the influence of bubbling time on the Cu-CO<sub>L</sub> peak area. The integrated peak area at  $-1.4$  V is normalized relative to the highest value of 10 min bubbling time (0.37). The figure clearly shows that after an initial increase, the Cu-CO<sub>L</sub> peak area decrease with CO bubbling time. The reason for the apparent reduction in the amount of Cu-CO<sub>L</sub> is possibly due to the molecules moving into a tilted position. Raval *et al.* [28] reported that adsorbed CO shifts from linear to tilted linear as  $\theta_{\text{CO}}$  increases. As *p*-polarized radiation probes vibrations, which have a dipole moment perpendicular to the surface, a tilt in Cu-CO<sub>L</sub> results in a decreased vector of the dipole moment which is perpendicular to the surface, hence the decrease in the Cu-CO<sub>L</sub> peak area with bubbling time. The conversion of Cu-CO<sub>L</sub> to more stable form of adsorbed CO is also expected at more concentrated CO solution ( $t_{\text{bubbling}}$  more than 10 min) which shows that the amount of Cu-CO<sub>L</sub> decreases whereas new form of adsorbed CO increases with holding time (spectra not shown). This will be discussed in future. This observation implies that as the  $\theta_{\text{CO}}$  increases (due to an increase in the amount of CO in solution

and the increased in potential holding time), another stable form of adsorbed CO is preferentially formed.

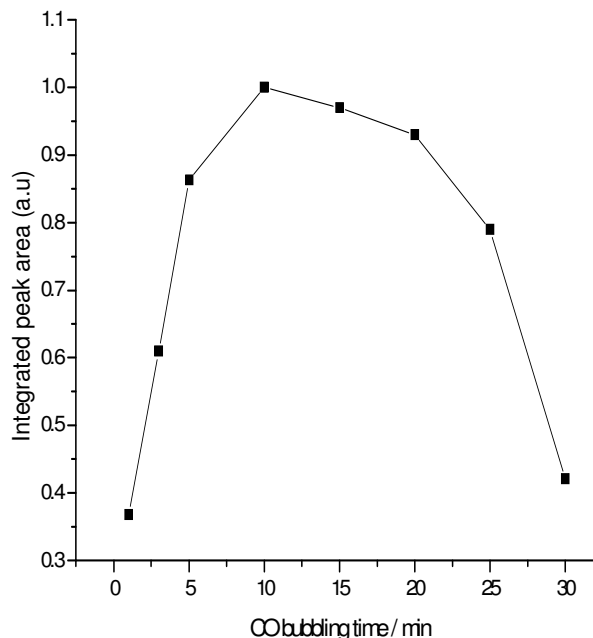


**Figure 6:** Integrated peak area of Cu-CO<sub>L</sub> at  $-1.4$  V versus CO concentration/CO bubbling time in buffered phosphate solution. SNIFTIR spectra are normalized relative to spectrum obtained at  $-0.8$  V for each set.

### Conclusion

The results show that the adsorption of CO process depends on the state of the copper surface either without or with potential polarization process. No adsorbed CO was observed without applying the potential to the electrode surface. Cu-CO<sub>L</sub> appeared immediately after the surface was polarized with the starting applied potential,  $E_{ASP}$  at high negative potential. It appeared in a small potentials range from  $-1.5$  to  $-1.0$  V. No Cu-CO<sub>L</sub> was observed at potential below  $-1.0$  V due to the competing process with the pre-adsorbed anions. It can be concluded that the interaction of CO on copper surface results in the adsorption of the molecular form. The appearance of Cu-CO<sub>L</sub> is dependent on the  $E_{ASP}$ , CO concentration and the  $\theta_{\text{CO}}$ . The results also show that the adsorption of CO on polycrystalline may occur at more than one binding sites, linearly bonded CO and may at multi-bonded CO.

### Acknowledgment

The authors would like to thank UKM-Malaysia for financial support and Dr. R.J. Nichol (U. Liverpool, UK) for useful discussions.

**References**

- 1 R. Hoffmann (1980) "*Solids and Surfaces: a chemist's view of bonding in extended structures*" Academic Press, N. York
- 2 R.R. Ford (1980) in "*Advances in Catalysis*," Vol. 21, D.E. Eley, H. Pines and P.B. Weisz (eds.), Academic Press, N. York
- 3 R. Maruca, T. Kusuma, V. Hicks and A. Companion (1990) *Surf. Sci.*, **236** 210
- 4 P. Hollins and J. Pritchard (1980) *Vibrational Spectroscopy of Adsorbates*, Series in "Chemical Physics", vol. 15, Chp. 8.
- 5 S. Pons (1983) *J. Electroanal. Chem.*, **150** 495
- 6 A. Bewick, S. Pons (1985) in R.J.H. Clark, R.E. Hester (eds.), *Advances in Infrared and Raman Spectroscopy*, Vol. 12 Chapter 1.
- 7 J. Salimon and M. Kalaji (2002) *Asean J. on Sci. and Tech. for Develop.*, in press.
- 8 Y. Hori, O. Koga, H. Yamazuki and T. Matsuo (1995), *Electrochim. Acta*, **40** 2617
- 9 Y. Hori, A. Murata, T. Tsukamoto, H. Wakebe, O. Koga and H. Yamazaki (1994), *Electrochim. Acta.*, **39** 2495
- 10 J. Pritchard and M.L. Sims (1970), *Trans. Faraday Soc.*, **66** 427
- 11 B.E. Hayden, K. Kretzschmar and A.M. Bradshaw (1985), *Surf. Sci.*, **155** 553
- 12 K. Horn, M. Hussian and J. Pritchard (1977), *Surf. Sci.*, **63** 244
- 13 J. Salimon and M. Kalaji (2002), *Malays. J. of Sci.*, in press
- 14 F. Stoop, F.J.C.M. Toolenor and V. Poniec (1981), *J. Chem. Soc.*, **1024**
- 15 S. Pinchas and I. Laulicht (1971), "*Infrared Spectra of Labelled Compounds*", Academic Press, London,
- 16 P. Hollins, K.J. Davies and J. Pritchard (1984), *Surf. Sci.*, **138** 75
- 17 P. Dumas, R.G. Tobin and P.L. Richards (1987), *Surf. Sci.*, **173** 79
- 18 M.W. Severson, C. Stuhlmann, I. Villegas and M.J. Weber (1995), *J. Chem. Phys.*, **103** 9832
- 19 C.S. Kim, W.J. Tornquist and C. Korzeniewski (1994), *J. Chem. Phys.*, **101** 9113
- 20 B.E. Hayden, K. Prince, D.P. Woodruff and A.M. Bradshaw (1983), *Surf. Sci.*, **133** 589
- 21 D.P. Woodruff, B.E. Hayden, K. Prince and A.M. Bradshaw (1982), *Surf. Sci.*, **123** 397
- 22 G. Herzberg (1945), "*Molecular Spectra and Molecular Structure*", Vol 1, 2<sup>nd</sup> Ed. Van Nostrand, N. York
- 23 J. Ambrose, R.G. Barradas and D.W. Shoesmith (1973), *J. Electroanal. Chem.*, **47** 65
- 24 M.R. Gennero de Chialvo, J.O. Zerbino, S.L. Marchiano and A.J. Arvia (1986), *J. Appl. Electrochem.*, **16** 517
- 25 J.M.M. Droog, C.A. Alderliesten, P.T. Alderliesten and G.A. Bootsma (1980), *J. Electroanal. Chem.*, **112** 387
- 26 C.H. Pyun and S.M. Park (1986), *J. Electrochem. Soc.*, **133** 2024
- 27 D. Armstrong, N.A. Hampson and R.J. Latham (1969), *J. Electroanal. Chem.*, **23** 361
- 28 R. Raval, S.F. Parker, M. E. Pemble, P. Hollins, J. Pritchard and M.A. Chester (1988) s, *Surf. Sci.*, **203** 353.

**Caption for Figures**

**Figure 1**

**Figure 2**

**Figure 3**

**Figure 4**

**Figure 5**

**Figure 6**

A large, empty rectangular box with a thin black border, occupying the lower half of the page. The text 'Figure 6' is positioned at the top-left corner of this box.